Icarus 426 (2025) 116362

Contents lists available at ScienceDirect

Icarus

journal homepage: www.elsevier.com/locate/icarus

Iron isotopes of Chang'e-5 soil and mineral components: Implications for post-eruption processes on lunar surface

Yiheng Li [a], Zaicong Wang [a,*], Yuqi Qian [b], Wen Zhang [a], Yantong Feng [c], Hong Liu [a], Keqing Zong [a], Qi He [a], Zhenbing She [a], Xiang Wu [a], Ming Li [a], Zhaochu Hu [a], Long Xiao [a], Yang Li [d], Frederic Moynier [e]

[a] State Key Laboratory of Geological Processes and Mineral Resources, School of Earth Sciences, China University of Geosciences, Wuhan 430074, China
[b] Department of Earth Sciences and Laboratory for Space Research, The University of Hong Kong, Hong Kong, China
[c] Gansu Key Laboratory of Mineral Resources in Western China, School of Earth Sciences, Lanzhou University, Lanzhou 730000, China
[d] Center for Lunar and Planetary Sciences, Institute of Geochemistry, Chinese Academy of Sciences, Guiyang 550081, China
[e] Universite de Paris Cite, Institut de Physique du Globe de Paris, CNRS, UMR 7154, 75005 Paris, France

ARTICLE INFO

Keywords:
Chang'e-5
Fe isotopes
Space weathering
Disequilibrium crystallization
Olivine

ABSTRACT

Due to rapid magma cooling and extensive space weathering, significant disequilibrium crystallization and secondary modification widely occur in lunar mare basalt after its eruption on the lunar surface. In this study, we conducted bulk and in-situ Fe isotope analyses to investigate the post-eruption processes on Chang'e-5 (CE-5) samples. The CE-5 soil shows a minor elevation of δ^{56}Fe value (~0.05 ‰) relative to the CE-5 basalt clasts. Correlations between Ni and Cu contents with δ^{56}Fe values suggest that the minor increase in the δ^{56}Fe from the CE-5 basalt to soil primarily occurred during evaporation caused by meteorite impacts. Such isotopic variation between CE-5 basalt and soils is notably lower than what is observed for Apollo samples and reflects the low maturity of CE-5 soils. This is consistent with the low Is/FeO value constrained by magnetic approaches. Therefore, measuring the δ^{56}Fe values of lunar soil is suitable to evaluate the degrees of maturity for lunar soils due to space weathering. In-situ analyses of δ^{56}Fe reveal significant variations in different grains of olivine (δ^{56}Fe: −0.57 to −0.17 ‰) and ilmenite (−0.06 to +0.42 ‰) and also in their interior (mainly for olivine). These δ^{56}Fe variations in minerals can be ascribed to the disequilibrium crystallization of lava flow and fast cooling, which is consistent with conclusions based on petrologic observations such as its extensive differentiation and silicate liquid immiscibility. Therefore, the post-eruption processes on the lunar surface could lead to significant variations in isotopic compositions at different scales of basalts, which in turn record the history of late-stage magma evolution and space weathering on the lunar surface.

1. Introduction

The lunar soil, which usually refers to the fine portion (<1 mm) of the regolith (Mckay et al., 1991), is a dynamic and complex layer of loose material covering the Moon's surface. It can serve as a valuable repository of information about the Moon's geological history and the processes shaping planetary surfaces in our solar system (Lucey, 2006). Understanding its composition and characteristic is pivotal for unraveling the complex post-eruption processes on the lunar surface, shedding light on analogous processes occurring on other airless planetary bodies.

The recent Chinese mission, Chang'e-5 (CE-5), has provided new opportunities to study the lunar soil. Given the young eruption age of CE-5 basalt (~2.0 Ga; Che et al., 2021; Li et al., 2021) and the high altitude of the landing site, which had not been previously sampled, understanding the maturity and the space weathering effects of CE-5 soil has garnered widespread interest. Space weathering encompasses the cumulative alteration of materials exposed to the space environment, with soil maturity serving as a metric to evaluate the degree of these effects (Pieters and Noble, 2016). Morris (1976) identified a strong correlation among the grain size, submicroscopic iron content, and exposure age of Apollo lunar soils, suggesting that soils with finer grain sizes, higher submicroscopic iron content and longer exposure ages may exhibit increased maturity. However, investigations of CE-5 lunar soil have revealed contradictions among these classic indicators, leading to

* Corresponding author.
E-mail address: zaicongwang@cug.edu.cn (Z. Wang).

https://doi.org/10.1016/j.icarus.2024.116362
Received 5 August 2024; Received in revised form 15 October 2024; Accepted 28 October 2024
Available online 29 October 2024

conflicting assessments of its maturity. For instance, the average grain size of CE-5 lunar soil ranges from 50 to 60 μm (Li et al., 2022a, 2022b), which is finer than the ~30 to 150 μm observed in Apollo lunar soils (Carrier et al., 1991; Heiken et al., 1973; McKay et al., 1974). In-situ visible and near-infrared (VNIR) data further support the classification of CE-5 lunar soil as mature. Conversely, Qian et al. (2024) determined the Is/FeO value (the intensity of the characteristic ferromagnetic resonance normalized to total iron content) of CE-5 lunar soil using magnetic approaches, placing it within the range of immature lunar soils (Morris, 1980). Additionally, the average exposure age of CE-5 lunar soil is 430 (±116) Ma (Li et al., 2023), comparable to that of Apollo mature soils (Joy et al., 2016), while the $(^3He/^4He)_{tr}$ and $(^{20}Ne/^{22}Ne)_{tr}$ values indicated that weak secondary processes have occurred. These discrepancies underscore the necessity for using other methods to determine the maturity of the CE-5 soils, such as Fe isotope ratios.

The pioneering work of Wiesli et al. (2003) found a significant positive correlation between the maturity of the Apollo lunar soils and Fe isotope ratios. The heavier Fe isotopes are enriched in the finer and more mature soils. Wang et al. (2012) reported an exceptionally high $\delta^{56}Fe$ value of up to 0.71 ‰ in the surface layer of plagioclase from Apollo regolith, which may reflect signals from nanophase iron particles (np-Fe^0). This suggested that progressive enrichment in the heavier Fe isotopes in lunar soil could result from the cumulative accumulation of $npFe^0$. These studies suggest that Fe isotope ratios could serve a robust tracer for unraveling the lunar soil's maturity. Using mare basalt as an example, if we have precise knowledge of the initial iron isotope composition of the basaltic precursor material, we can assess the maturity of the lunar soil based on the observed elevation in iron isotopes. According to previous studies, the majority of the material of the CE-5 soil is from the local unit with limited exotic components, regardless of the depth of the CE-5 soil (Qian et al., 2021; Wang et al., 2024; Zeng et al., 2023; Zong et al., 2022). The straightforward geological setting gives a significant chance to directly compare the Fe isotopes of lunar soil and underlying basalt, shedding light on the space weathering processes and the effects on the young lunar soil.

Recent studies have found significant Fe—Mg inter-diffusion in CE-5 lunar soil, which has been attributed to meteorite impact events (Shi et al., 2024; Zhang et al., 2024). However, significant isotopic fractionation could also happen during fast cooling and disequilibrium crystallization of lunar magma lava (Oeser et al., 2015; Tian et al., 2020a, 2020b). Given the highly evolved features of CE-5 basalt, such as zoned pyroxene and silicate liquid immiscibility (SLI) (He et al., 2022; Jiang et al., 2023; Wang et al., 2023), different minerals of CE-5 basalt present an opportunity to investigate the disequilibrium fractionation of isotopes on the Moon.

In this study, we measured the bulk iron isotopes of CE-5 scooped soil and drill core, along with two agglutinates. Our aim is to elucidate the Fe isotope composition in different components on CE-5 landing site and understand the maturity and post-eruption processes of the CE-5 lunar soil.

2. Samples and methods

2.1. Bulk iron isotopic analyses

Two batches (200 mg CE5C0400 and 400 mg CE5C0600) of the scooped CE-5 lunar soil and one batch (100 mg CE5Z0906YJ, from a depth of ~10 cm) from the drill core were obtained from the China National Space Administration Agency. Importantly, magnetic measurements have been conducted on CE5C0600 by Qian et al. (2024), which is useful to compare with the Fe isotope ratios. Eight sub-samples from scooped soil, weighing between 2 and 6 mg, and three sub-samples from the drilled lunar soil, weighing between 2 and 4 mg, were analyzed for bulk compositions of major and trace elements and $\delta^{56}Fe$ in this study (Table S1). Additionally, two agglutinates (0.8 mg and 1.15 mg) were included in the analysis. The bulk chemical compositions of these soil subsamples and agglutinates indicate that most elements, except Ni and Mo, are relatively homogeneous (Wang et al., 2024; Zong et al., 2022). The sample digestion and measurement procedures have been well described by Zong et al. (2022). After major and trace elements analysis, the leftover solutions of the soil and agglutinates were used for Fe isotope analyses in this study in the State Key Laboratory of Geological Processes and Mineral Resources (GPMR) at China University of Geoscience (Wuhan), utilizing an established protocol (Lei et al., 2022).

Pre-cleaned AG-MP-1 M anion resin was utilized to achieve separation of Fe. Fe isotope ratios were measured using a Nu Plasma 1700 multi-collector inductively-coupled-plasma mass-spectrometry (MC-ICP-MS) and are reported in standard δ-notation in permil relative to IRMM014. The measured $\delta^{56}Fe$ values of reference standards (GSB-USTC, BHVO-2 and BCR-2) in this study are in agreement with the recommended values (Craddock and Dauphas, 2011; He et al., 2015) (Table S1) and the long-term external precision of $\delta^{56}Fe$ is better than 0.03 ‰ (2SD) (Lei et al., 2022).

2.2. In-situ Fe isotopic analysis of olivine and ilmenite

Several mineral fragments (olivine and ilmenite) and basalt clasts (typically >100 μm) were manually separated from the lunar soil and mounted in Araldite 2020 epoxy resin and polished. We selected several olivines and some ilmenites (from both basaltic clasts and olivine fragments) for in situ-iron isotope analysis. All of the in-situ isotopic analyses in this study were conducted with an ESI NWR FemtoUC femtosecond laser ablation system (New Wave Research, Fremont, CA, USA) coupled to a Neptune Plus MC-ICP-MS instrument (Thermo Fisher Scientific, Germany) at the GPMR.

For in-situ Fe isotope analysis of olivine, the laser ablation system operated in single-spot mode with a spot size of 40 μm. Ultrapure water was introduced into the ICP to suppress the matrix effect during the Fe isotope analysis. A detector array of Faraday cups was set to acquire the ion beams of ^{53}Cr, ^{54}Fe, ^{56}Fe, ^{57}Fe, ^{58}Fe, and ^{60}Ni. ^{53}Cr and ^{60}Ni were monitored and used for the isobaric interference correction of ^{54}Cr on ^{54}Fe and ^{58}Ni on ^{58}Fe with a $^{54}Cr/^{53}Cr$ ratio of 0.2489 and $^{60}Ni/^{58}Ni$ ratio of 0.3852, respectively. Given the high FeO (30–60 wt%) and low Cr (100–500 μg/g) content of olivine in CE-5 basalt (Su et al., 2023), the interference could be corrected. The SSB (sample-standard bracketing) method was employed for mass fractionation correction. The $^{56}Fe/^{54}Fe$ and $^{57}Fe/^{54}Fe$ ratios were converted to the standard IRMM-014. The reference material was used as an external standard, while pyite Aa018, PAS-Py600 and chalcopyrite PAS-Cpy400 were analyzed repeatedly as unknown samples to evaluate the reliability of non-matrix-matched correction. The average $\delta^{56}Fe$ values of Aa018, PAS-Py600 and PAS Cpy400 are 0.52 ± 0.04 ‰, 0.19 ± 0.03 ‰ and − 0.05 ± 0.07 ‰, respectively, which is in agreement with the reference value within uncertainty (Table S2, Fig. S1) (Feng et al., 2022). Offline data processing was performed using the Iso-Compass software (Zhang et al., 2020).

The Fe isotopic analysis of ilmenite was operated with a spot of 40 μm, for a laser energy density of 2 J cm-2 and a low repetition rate of 5 Hz. Standard two-volume ablation cell (TV-2) and wet plasma conditions was used to reduce isotopic fractionation. A standard sampler cone combined with an X skimmer cone (S + X cones) was employed to obtain a higher sensitivity and a detailed method can be found in Xu et al. (2022). The results are finally expressed relative to IRMM-014. Ilmenite CZE2, HER16 and GER16 were used as the reference materials, whose $\delta^{56}Fe$ value is in agreement with the reference value within uncertainty (Table S3, Fig. S2).

3. Results

The Fe isotope composition of aliquots of 12 subsamples (seven scooped soils, three drill soils and two agglutinates) are reported in

Table S1. These results will be compared with the Fe isotope composition of basaltic clasts from Jiang et al. (2023). The δ^{56}Fe values of scooped soils are homogeneous (+0.16 ± 0.02 ‰, 2SD, n = 8), which is similar to the drill soils (+0.14 ± 0.04 ‰, 2SD, n = 3) (Fig. 1). One agglutinate displays the highest δ^{56}Fe values of 0.22 ± 0.03 ‰, while the other is comparable to scooped soils (0.17 ± 0.02 ‰). Our results are also consistent with the δ^{56}Fe values of the CE-5 soil of different sizes reported by Shi et al. (2024) (Fig. 2). The Ni and Cu content of these samples have been reported in Wang et al. (2024). They demonstrate a strong correlation with δ^{56}Fe values (Fig. 3).

Two basaltic clasts (Fig. 4) and several mineral fragments were selected for in-situ Fe isotope analyses. The δ^{56}Fe values of olivine and ilmenite exhibit large variations, ranging from −0.57 to −0.17 ‰ and −0.06 to +0.42 ‰, respectively (Fig. 5). Considering the chemical zonation observed in olivine in CE-5 basalts (Tian et al., 2023; Wang et al., 2023), we selected four large olivines (~200 μm) to analyze the iron isotope composition of the core and rim. Overall, these olivines demonstrate intragrain variation in δ^{56}Fe with heavier core and lighter rim. The Fe isotope composition of ilmenites from three basaltic fragments also shows a large range, which are −0.05 to 0.10 ‰, 0.21 to 0.42 ‰ and − 0.6 to 0.28 ‰, respectively. The Fe isotope of ilmenites is heavier than olivines, consistent with mineral separate studies from Craddock et al. (2010).

4. Discussion

4.1. Space weathering effects on the CE-5 soil

Owing to the long-time sputtering and mixing during the (micro) meteorite impact events, lunar soils are compositionally modified in terms of several aspects (Lucey, 2006): 1) contamination by exotic components, including meteorites and materials from other geological units (e.g., Korotev et al., 2011); 2) enrichment or melting of specific minerals (e.g., plagioclase and ilmenite) in soil (Cintala, 1992; Horz et al., 1984; Taylor et al., 2010); and 3) evaporation and condensation effect during space weathering. In these cases, we will consider the formation of the CE-5 lunar soil and potential Fe isotopic fractionation during these processes.

Taylor et al. (2001) found that with the increasing of maturity, the concentrations of FeO, MgO, and TiO_2 decrease, while the concentrations of CaO, Na_2O, and Al_2O_3 increase. They interpreted these results in terms of a differential melting sequence for lunar soils: plagioclase > pyroxene ≫ ilmenite (Horz et al., 1984; Taylor et al., 2001). Regarding CE-5 samples, the soils are enriched in CaO, Al_2O_3 and MgO, depleted in FeO and TiO_2 (Fig. 2a, b and c) compared to the basaltic clasts. These results suggest that plagioclase was preferentially shattered into the soils compared to ilmenite. The Cr concentration is similar in both basalt clasts and soils (Fig. 2d), indicating a consistent abundance of pyroxene. Craddock et al. (2010) reported that ilmenite separate is enriched in heavy isotopes. Therefore, CE-5 soil was expected to have low δ^{56}Fe values with the depletion of TiO_2; however, such prediction is contrary to our results (Fig. 2a). As a result, the redistribution of minerals between soil and basalts is unlikely to be the primary cause of the Fe isotopic difference (Shi et al., 2024).

Zong et al. (2022) evaluated the effects of exotic impact ejecta and meteoritic materials in CE-5 bulk soil composition. They suggested minimal contamination (<5 %) by exotic materials from other geological units, consistent with previous studies on impact glass beads (2 %; Yang et al., 2022) and clasts in CE-5 soil (~0.2 %; Zeng et al., 2023). If isotopically heavy components were added to the CE-5 soil, they would likely originate from high-Ti basalts (Poitrasson et al., 2019). However, the lower Ti concentration observed in CE-5 soil (Fig. 2a) compared to basalt clasts does not support this hypothesis. The meteoritic contribution to CE-5 lunar soil is estimated to be around 1 wt% based on Ni and Ir contents (Yao et al., 2022; Zong et al., 2022). Although the Fe isotopic composition of the soil increases with increasing Ni content (Fig. 3a), the addition of meteorites may not be the primary factor contributing to the elevated δ^{56}Fe value. This is because both chondritic and iron meteorites typically exhibit lower δ^{56}Fe values compared to lunar soil (Williams et al., 2006).

In these cases, the strong positive correlation between Ni content and δ^{56}Fe values (Fig. 2d) may indicate that as space weathering intensifies, the fractionation of Fe isotopes becomes increasingly pronounced. Thus, our results from the young CE-5 samples further indicate that the space weathering process plays a significant role in altering the Fe isotopic composition of lunar soil (Wang et al., 2012; Wiesli et al., 2003).

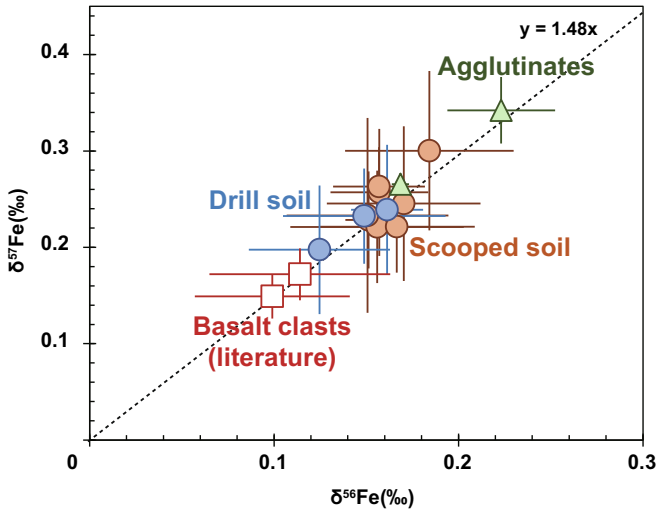

Fig. 1. Plot of δ^{57}Fe vs. δ^{56}Fe values for the CE-5 scooped, drill and agglutinates. Fe isotopes of basalt clasts from Jiang et al. (2023) (red hollow square) are used for comparison. The lunar soils from the surface and deeper level (~10 cm) are isotopically heavier than basalt clasts, and the agglutinates have the heaviest Fe isotope composition. (For interpretation of the references to colour in this figure legend, the reader is referred to the web version of this article.)

4.2. Low maturity of CE-5 lunar soil

Lunar soil maturity has typically been assessed through various indices, including mean grain size, agglutinate abundance, solar wind abundance, and surface-correlated $npFe^0$ (Housley et al., 1975; Morris, 1976). Since $npFe^0$ is a direct product of space weathering (Pieters and Noble, 2016; Shen et al., 2024) and Is/FeO reflects the $npFe^0$ content in lunar soil, we thus follow the well-established way and consider Is/FeO to be a decisive indicator for evaluating the lunar soil maturity (e.g., Is/FeO < 30 for an immature soil but >60 for a mature soil, Fig. 6; (Morris, 1980)). However, the fine grain size (Li et al., 2022a; Cao et al., 2022) and its long exposure age of CE-5 (Li et al., 2023), which are comparable to that of Apollo mature soils, present a contradiction with the lower Is/FeO value (Qian et al., 2024). The reasons behind these discrepancies, as well as the true maturity of the soil, are the key concerns of our study.

In this study, we observed an elevation of ~0.05 ‰ in the δ^{56}Fe value between CE-5 scooped soil and basalt clasts. This increase in Fe isotope ratios is relatively modest compared to the values seen in Apollo soil samples (Fig. 6). According to Fig. 6, when lunar soil reaches a maturity level of submature (Is/FeO of 30 to 60) and mature (Is/FeO > 60), the δ^{56}Fe values increase by ~0.05 ‰ and ~ 0.1 ‰, respectively. Therefore, the increase of ~0.05 ‰ in δ^{56}Fe for CE-5 lunar soil compared to basalt indicates that it still falls within the category of immature or submature lunar soil. The slight increase in δ^{56}Fe of the CE-5 soil aligns with the lower Is/FeO value (Qian et al., 2024), supporting the low maturity of CE-5 lunar soil. The identical Fe isotope composition from different batches and depths of the CE-5 soil (Figs. 1 and 2) indicates consistent degrees of space weathering at both surface and deeper levels (~10 cm),

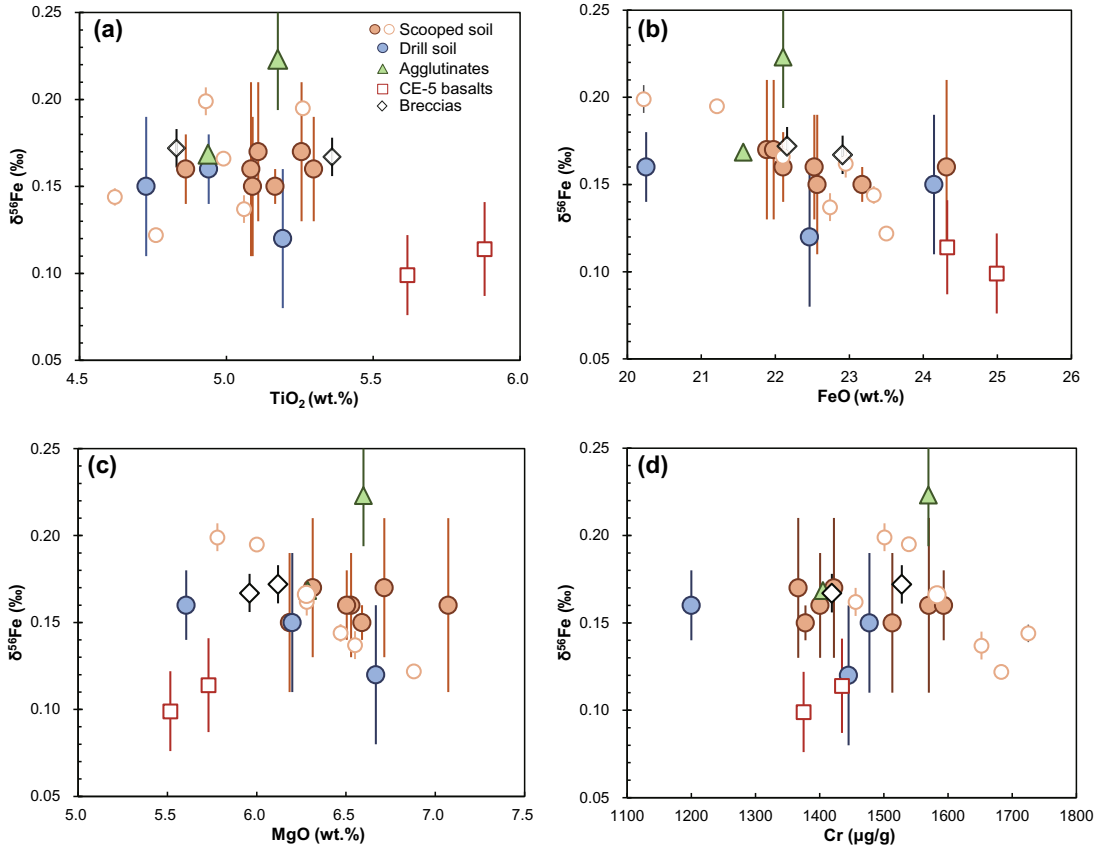

Fig. 2. The variation of δ^{56}Fe values with TiO_2 (a), FeO (b), MgO (c) and Cr (d) in basalt clasts, scooped and drill soils, and agglutinates. Fe isotope composition of sieved soils (orange hollow circle) and breccias (black hollow diamond) are used for comparison (Shi et al., 2024). The δ^{56}Fe values of soils from different batches and depths (surface and drill core) are comparable and consistently heavier than basalt clasts. The differences in ilmenite, olivine and pyroxene does not have a major influence on the Fe isotope fractionation.

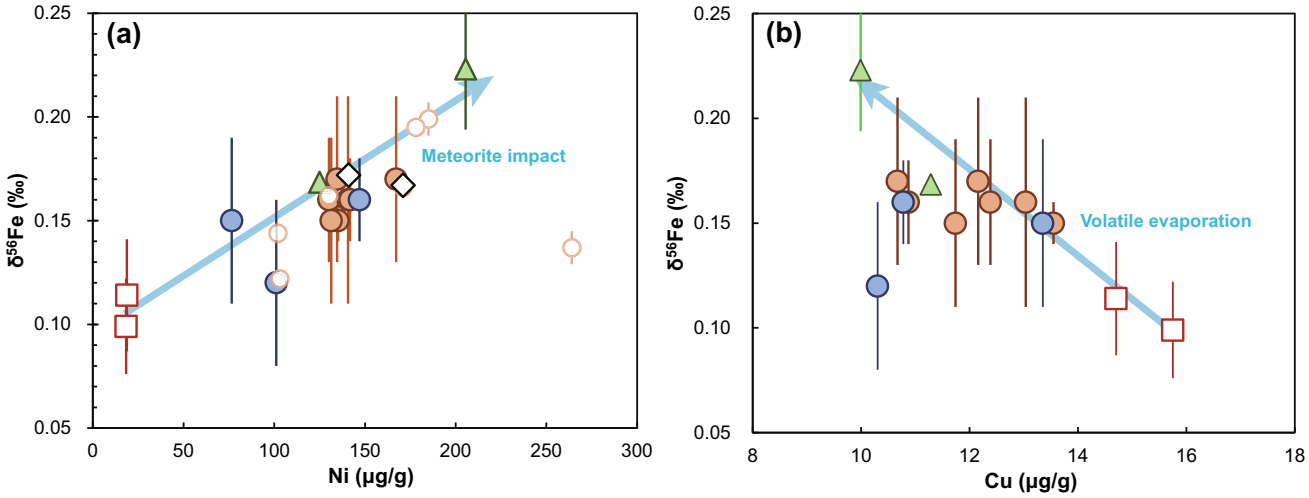

Fig. 3. (a) The δ^{56}Fe values are positively correlated with the Ni content. It indicates that the variations in the Fe isotope composition in lunar soil is related to meteorite impacts. (b) A negative correlation between δ^{56}Fe and Cu content suggests that volatile evaporation is the main controller of Fe isotope fractionation in CE-5 lunar soil.

further supporting the homogeneous chemical composition of CE-5 soil (Wang et al., 2024).

Interestingly, δ^{56}Fe in Apollo lunar soils at low maturity (~0.05 ‰) are even lower than theirs primary mare basalt (Low-Ti basalt at 0.076 ‰; High-Ti basalt at 0.184 ‰; Poitrasson et al., 2019). This observation suggests that while the overall Fe isotope composition of Apollo lunar soils increases with maturity, lighter Fe isotopic components may still be introduced. This aligns with previous findings of lighter K and Zn isotope deposits on the lunar surface (Day et al., 2017; Tian et al., 2020a, 2020b).

Wang et al. (2012) proposed that the enrichment in the heavier Fe isotopes in the lunar soil is largely due to the deposits of np-Fe^0, whose

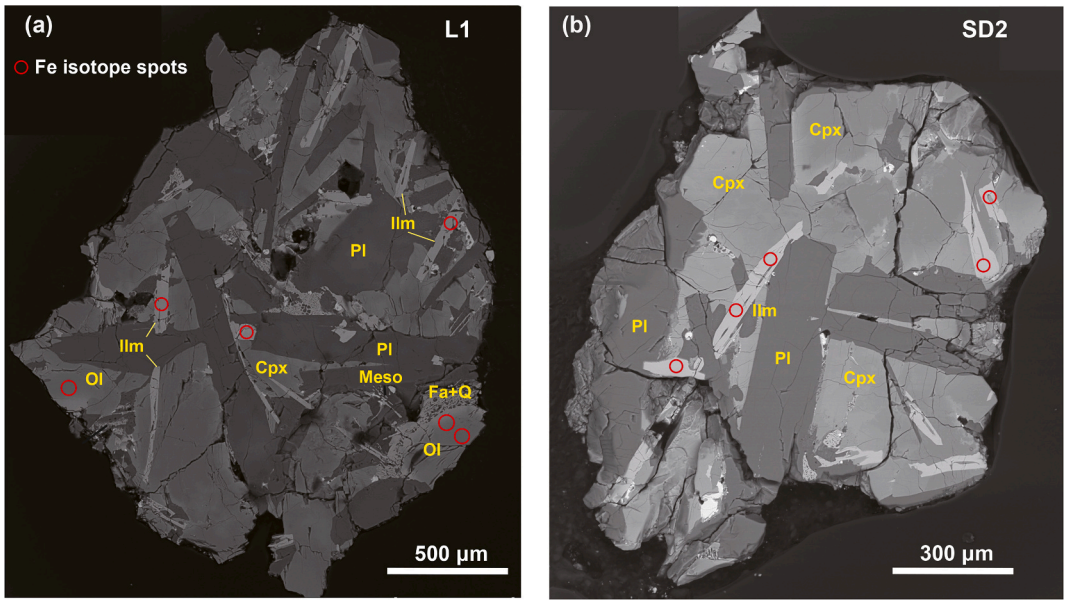

Fig. 4. BSE images of two basalt clasts chosen for in-situ Fe isotope analyses. Red circles are the laser spot of the Fe isotope measurements. (For interpretation of the references to colour in this figure legend, the reader is referred to the web version of this article.)

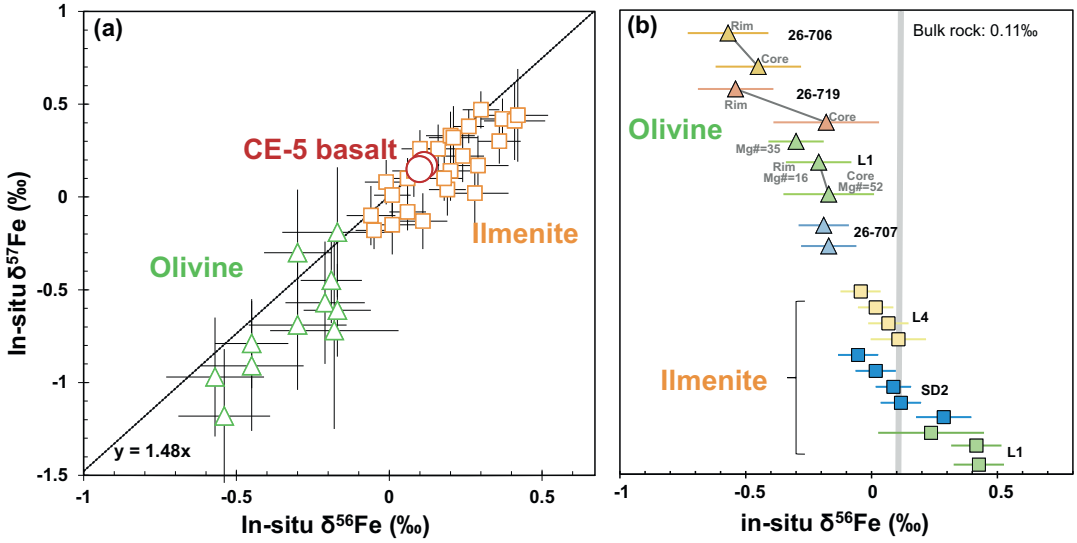

Fig. 5. Plot of δ^{57}Fe vs. δ^{56}Fe for the ilmenite and olivine. The Fe isotope composition of ilmenite is significantly heavier than olivine. The Fe isotopes of basalt clasts are used for comparison.

δ^{56}Fe values could be up to 0.71 ‰. However, most np-Fe^0 in CE-5 soil may have been generated in disproportional reaction or decomposition of fayalite (Li et al., 2022a; Guo et al., 2022; Xian et al., 2023). These processes are unlikely to fractionate Fe isotopes at the bulk soil scale. Instead, the δ^{56}Fe of the CE-5 soil shows broadly negative trends with moderately volatile elements such as Cu (Figs. 3b). The result likely suggests that the elevation of Fe isotopes in the CE-5 soil and agglutinates is more likely controlled by volatile evaporation during meteorite impacts (Figs. 3a and b).

The Ni (130-167 μg/g; Zong et al., 2022) and Ir (360–760 ng/g; Yao et al., 2022) contents in CE-5 lunar soil suggest a meteoritic contribution of ~1 wt%, which is significantly lower than the 1.5–2 wt% contribution observed in mature Apollo lunar soils. This indicates that, despite the exposure age of CE-5 lunar soil being similar to that of Apollo mature soils (Li et al., 2023), the CE-5 may have experienced lower flux of meteoritic impacts, resulting in a lower degree of maturity. This reduction in impact events may be associated with the decreased bombardment experienced by the Earth-Moon system after 3.5 Ga (Xie et al., 2020). Therefore, exposure age may not be the key indicator of lunar soil maturity. Instead, given the high FeO content of lunar soil and the rather simple measurement of Fe isotope ratios, the Fe isotope composition of the lunar soils could serve as a fast and useful indicator to evaluate their maturity, which reconcile with Is/FeO index.

4.3. *Disequilibrium fractionation of Fe isotope in and between minerals*

Our study reveals a wide range of δ^{56}Fe values in both olivine and ilmenite, with olivine consistently showing lighter isotope composition compared to ilmenite (Fig. 5a and b). Previous studies in lunar samples have indicated minimal Fe isotope fractionation in mare basalts during magmatic differentiation due to reduced conditions (Liu et al., 2010; Prissel et al., 2024; Sossi and Moynier, 2017). According to Sossi and

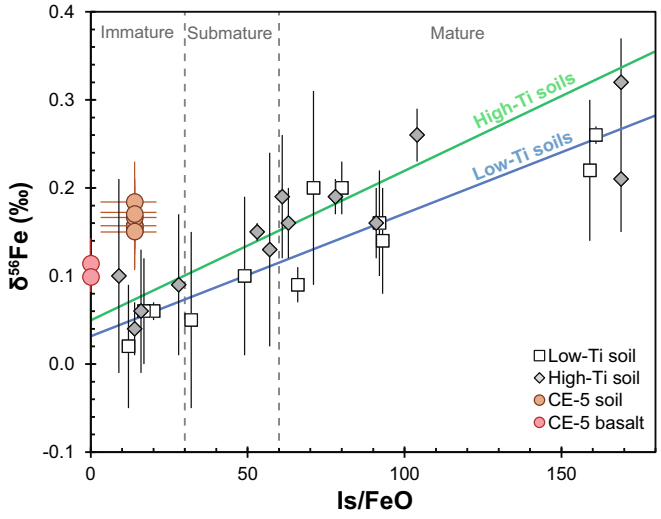

Fig. 6. δ^{56}Fe variation with Is/FeO in CE-5 and Apollo soils. A strong correlation exists between δ^{56}Fe and Is/FeO in Apollo soil (Wiesli et al., 2003). The elevation of δ^{56}Fe between CE-5 soil and basalt is lower than Apollo soil.

O'Neill (2017), the Fe—O bond lengths in fayalite and ilmenite are comparable, suggesting limited fractionation in δ^{56}Fe during equilibrium conditions. Therefore, the observed difference of ~0.5 ‰ in δ^{56}Fe between ilmenite and olivine in CE-5 samples may indicate a disequilibrium situation.

Significant Fe isotope fractionation between silicates and Fe—Ti oxides has been documented in terrestrial Fe—Ti oxide ores (Cao et al., 2019; Liu et al., 2014). This fractionation is attributed to factors such as oxygen fugacity influencing the crystallization order of Fe—Ti oxides (Liu et al., 2014) or the in situ crystallization of different phases of Fe—Ti oxides (magnetite and ilmenite) from Fe-rich melts (Cao et al., 2019). However, such conditions unlikely occurred in CE-5 basalts. Our interpretation leans towards disequilibrium conditions resulting from rapid cooling and extensive magma evolution as the primary drivers of Fe isotope fractionation between ilmenite and olivine. This conclusion is consistent with the widely observed SLI phenomenon in CE-5 basalt, indicating that many fayalite and ilmenite grains likely formed within the mesostasis (He et al., 2022; Jiang et al., 2023). Additionally, extreme chemical zoning in olivine and pyroxene (Fig. 4a and b) with olivine cores typically showing high Fo values (60–65) and rims adjacent to late-stage mesostasis pockets showing lower values (Luo et al., 2023; Su et al., 2023), further indicates high degrees of disequilibrium during CE-5 magma cooling. We observed isotopically heavier cores in most olivines, along with significant variations in Fe isotopes of ilmenite (Fig. 5b), suggesting a role of diffusion processes. Previous studies on Mg—Fe isotopes in CE-5 lunar soils and agglutinates have highlighted impact-induced diffusion-driven fractionation (Shi et al., 2024; Zhang et al., 2024). While we do not rule out the possibility that impact processes may lead to Mg—Fe diffusion in lunar soil particles, potentially affecting their Fe isotope composition, the basalt clasts analyzed in this study exhibit minimal signs of such impact alteration (Fig. 4a and b). This suggests that diffusion-driven fractionation likely occurred at the mineral scale, possibly due to chemical gradients between olivine and ilmenite in conjunction with surrounding segregated melts (Pernet-Fisher et al., 2019; Tian et al., 2020a, 2020b), or through inter-grains Fe—Mg exchange.

In conclusion, our study has identified substantial Fe isotope fractionation in CE-5 basalt clasts, primarily attributed to disequilibrium crystallization during rapid cooling and chemical-driven diffusion of mineral interior. These processes are very common in lunar samples (e.g. Day et al., 2006; Jolliff, 1998; Pernet-Fisher et al., 2019) and underscore the important effects of post-eruption processes for stable isotope fractionation in intragrain or inter-grain scales, for example also for the inconsistencies in Fe isotopes between minerals in Craddock et al. (2010). However, such fractionation of Fe isotopes occurs mainly at the mineral scale and could have a limited effect on the overall isotopic composition of the bulk rock.

5. Conclusions

Our study presents that the CE-5 scooped and drilled samples have similar average δ^{56}Fe values of +0.16 ± 0.02 ‰ (2SD, $n = 8$) and + 0.14 ± 0.04 ‰ (2SD, $n = 3$), regardless of the soil grain size (from <56 μm to >180 μm , Shi et al., 2024). The soils show a minor elevation of δ^{56}Fe (~0.05 ‰) relative to the CE-5 basalt clasts (~0.11 ‰, Jiang et al., 2023), which suggests the immaturity of CE-5 soil after its exposure to surface. We propose that the evaporation process indued by meteorite impacts appears to play a major role for such increase in δ^{56}Fe of CE-5 soil. Our results suggest that the grain size and exposure age may not be a decisive indicator of the maturity of lunar soil, while the Fe isotope ratios could serve as a convenient method, complementary to the Is/FeO index.

A wide variation in Fe isotope compositions was also observed in olivine and ilmenite in CE-5 basaltic clasts and monomineralic fragments, which cannot be attributed to magmatic differentiation alone. We propose that the substantial fractionation of Fe isotopes in olivine and ilmenite resulted from disequilibrium fractionation between minerals and late-stage immiscible melts formed during the SLI process as the magma was fast cooling. Given the widespread occurrence of SLI in lunar mare basalt, this disequilibrium fractionation of Fe isotopes could be a common phenomenon on the Moon.

CRediT authorship contribution statement

Yiheng Li: Writing – review & editing, Writing – original draft, Methodology, Data curation, Conceptualization. **Zaicong Wang:** Writing – review & editing, Writing – original draft, Investigation, Data curation, Conceptualization. **Yuqi Qian:** Investigation, Conceptualization. **Wen Zhang:** Methodology. **Yantong Feng:** Methodology. **Hong Liu:** Methodology. **Keqing Zong:** Project administration. **Qi He:** Formal analysis. **Zhenbing She:** Resources. **Xiang Wu:** Resources. **Ming Li:** Methodology. **Zhaochu Hu:** Resources. **Long Xiao:** Resources. **Yang Li:** Conceptualization. **Frederic Moynier:** Conceptualization.

Declaration of competing interest

The authors declare that they have no known competing financial interests or personal relationships that could have appeared to influence the work reported in this paper.

Acknowledgments

We appreciate all staff of the Chang'e-5 mission for returning samples and the China National Space Administration (CNSA) for providing samples (CE5C0400, CE5C0600 and CE5Z0906YJ). This work was funded by the National Natural Science Foundation of China (No. 42241156 and 42273023).

Appendix A. Supplementary data

Supplementary data to this article can be found online at https://doi.org/10.1016/j.icarus.2024.116362.

Data availability

Data will be made available on request.

References

Cao, Y., Wang, C.Y., Huang, F., Zhang, Z., 2019. Iron isotope systematics of the Panzhihua mafic layered intrusion associated with Giant Fe-Ti oxide deposit in the Emeishan large Igneous Province, SW China. J. Geophys. Res. Solid Earth 124, 358–375. https://doi.org/10.1029/2018JB016466.

Cao, K., Dong, M., She, Z., Xiao, Q., Wang, X., Qian, Y., Li, Y., Wang, Z., He, Q., Wu, X., Zong, K., Hu, Z., Xiao, L., 2022. A novel method for simultaneous analysis of particle size and mineralogy for Chang'E-5 lunar soil with minimum sample consumption. Sci. China Earth Sci. https://doi.org/10.1007/s11430-022-9966-5.

Carrier, W.D., Olhoeft, G., Mendell, M., 1991. Physical Properties of the Lunar Surface, in: Lunar Sourcebook. Cambridge University Press, Cambridge, UK.

Che, X., Nemchin, A., Liu, D., Long, T., Wang, C., Norman, M.D., Joy, K.H., Tartese, R., Head, J., Jolliff, B., Snape, J.F., Neal, C.R., Whitehouse, M.J., Crow, C., Benedix, G., Jourdan, F., Yang, Z., Yang, C., Liu, J., Xie, S., Bao, Z., Fan, R., Li, D., Li, Z., Webb, S. G., 2021. Age and composition of young basalts on the Moon, measured from samples returned by Chang'e-5. Science, eabl7957. https://doi.org/10.1126/science.abl7957.

Cintala, M., 1992. Impact-induced thermal effects in the Lunar and Mercurian regolith. J. Geophys. Res. 97. https://doi.org/10.1029/91JE02207.

Craddock, P.R., Dauphas, N., 2011. Iron isotopic compositions of geological reference materials and chondrites. Geostand. Geoanal. Res. 35, 101–123. https://doi.org/10.1111/j.1751-908X.2010.00085.x.

Craddock, P.R., Dauphas, N., Clayton, R.N., 2010. Mineralogical control on iron isotopic fractionation during lunar differentiation and magmatism. Lunar Planet. Sci. Conf. 1230.

Day, J.M.D., Taylor, L.A., Floss, C., Patchen, A.D., Schnare, D.W., Pearson, D.G., 2006. Comparative petrology, geochemistry, and petrogenesis of evolved, low-Ti lunar mare basalt meteorites from the LaPaz Icefield, Antarctica. Geochim. Cosmochim. Acta 70, 1581–1600 doi:10/dd4455.

Day, J.M.D., Moynier, F., Shearer, C.K., 2017. Late-stage magmatic outgassing from a volatile-depleted moon. Proc. Natl. Acad. Sci. USA 114, 9547–9551 doi:10/ghqm72.

Feng, Y., Zhang, W., Hu, Z., Luo, T., Li, M., Liu, Y., Liu, H., Li, Q., 2022. A new synthesis scheme of pyrite and chalcopyrite reference materials for *in situ* iron and sulfur isotope analysis using LA-MC-ICP-MS. J. Anal. At. Spectrom. 37, 551–562. https://doi.org/10.1039/D1JA00392E.

Guo, Z., Li, C., Li, Y., Wen, Y., Wu, Y., Jia, B., Tai, K., Zeng, X., Li, X., Liu, J., Ouyang, Z., 2022. Sub-microscopic magnetite and metallic iron particles formed by eutectic reaction in Chang'E-5 lunar soil. Nat. Commun. 13, 7177. https://doi.org/10.1038/s41467-022-35009-7.

He, Y., Ke, S., Teng, F.-Z., Wang, T., Wu, H., Lu, Y., Li, S., 2015. High-precision Iron isotope analysis of geological reference materials by high-resolution MC-ICP-MS. Geostand. Geoanal. Res. 39, 341–356. https://doi.org/10.1111/j.1751-908X.2014.00304.x.

He, Q., Li, Y., Baziotis, I., Qian, Y., Xiao, L., Wang, Z., Zhang, W., Luo, B., Neal, C.R., Day, J.M.D., Pan, F., She, Z., Wu, X., Hu, Z., Zong, K., Wang, L., 2022. Detailed petrogenesis of the unsampled Oceanus Procellarum: the case of the Chang'e-5 mare basalts. Icarus 383, 115082. https://doi.org/10.1016/j.icarus.2022.115082.

Heiken, G.H., McKay, D.S., Fruland, R.M., 1973. Apollo 16 soils: grain size analyses and petrography. Lunar Planet. Sci. Conf. Proc. 4, 251.

Horz, F., Cintala, M., See, T., Cardenas, F., Thompson, T., 1984. Grain size evolution and fractionation trends in an experimental regolith. Proc. Lunar Planet. Sci. Conf. 15. https://doi.org/10.1029/JB089iS01p0C183.

Housley, R.M., Cirlin, E.H., Goldberg, I.B., Crowe, H., Weeks, R.A., Perhac, R., 1975. Ferromagnetic resonance as a method of studying the micrometeorite bombardment history of the lunar surface. Lunar Planet. Sci. Conf. Proc. 3, 3173–3186.

Jiang, Y., Kang, J., Liao, S., Elardo, S.M., Zong, K., Wang, S., Nie, C., Li, P., Yin, Z., Huang, F., Hsu, W., 2023. Fe and mg isotope compositions indicate a hybrid mantle source for young Chang'E 5 Mare basalts. ApJL 945, L26. https://doi.org/10.3847/2041-8213/acbd31.

Jolliff, B.L., 1998. Large-scale separation of K-frac and REEP-frac in the source regions of Apollo impact-melt Breccias, and a revised estimate of the KREEP composition. Int. Geol. Rev. 40, 916–935. https://doi.org/10.1080/00206819809465245.

Joy, K., Crawford, I., Curran, N., Zolensky, M., Fagan, A., Kring, D., 2016. The moon: an archive of small body migration in the solar system. Earth Moon Planet. 118. https://doi.org/10.1007/s11038-016-9495-0.

Korotev, R.L., Jolliff, B.L., Zeigler, R.A., Seddio, S.M., Haskin, L.A., 2011. Apollo 12 revisited. Geochim. Cosmochim. Acta 75, 1540–1573. https://doi.org/10.1016/j.gca.2010.12.018.

Lei, Y., Li, M., Wang, Z., Zhu, Y., Hu, Z., Li, Y., Chai, X., 2022. Iron isotopic measurement using large-geometry high-resolution multi-collector inductively coupled plasma mass spectrometer. At. Spectrosc. 43, 214–222. https://doi.org/10.46770/AS.2022.111.

Li, Q.-L., Zhou, Q., Liu, Y., Xiao, Z., Lin, Y., Li, J.-H., Ma, H.-X., Tang, G.-Q., Guo, S., Tang, X., Yuan, J.-Y., Li, J., Wu, F.-Y., Ouyang, Z., Li, C., Li, X.-H., 2021. Two-billion-year-old volcanism on the moon from Chang'e-5 basalts. Nature 600, 54–58. https://doi.org/10.1038/s41586-021-04100-2.

Li, Chen, Guo, Z., Li, Y., Tai, K., Wei, K., Li, X., Liu, J., Ma, W., 2022a. Impact-driven disproportionation origin of nanophase iron particles in Chang'e-5 lunar soil sample. Nat. Astron. 6, 1156–1162. https://doi.org/10.1038/s41550-022-01763-3.

Li, Chunlai, Hu, H., Yang, M.-F., Pei, Z.-Y., Zhou, Q., Ren, X., Liu, B., Liu, D., Zeng, X., Zhang, G., Zhang, H., Liu, J., Wang, Q., Deng, X., Xiao, C., Yao, Y., Xue, D., Zuo, W., Su, Y., Wen, W., Ouyang, Z., 2022b. Characteristics of the lunar samples returned by the Chang'E-5 mission. Natl. Sci. Rev. 9, nwab188. https://doi.org/10.1093/nsr/nwab188.

Li, J., Li, Z., Huang, Z., Li, T., Guo, D., Liu, H., Fan, G., Qin, M., Lei, L., Zhou, X., Wang, H., Wang, K., Gao, X., Yu, A., Liu, R., Zhang, J., Deng, L., He, S., Wu, Y., Qiu, L., 2023. Weak influence of the secondary surface processes on the regolith of Chang'E-5 landing site. Commun. Earth Environ. 4, 1–9. https://doi.org/10.1038/s43247-023-00937-9.

Liu, Y., Spicuzza, M.J., Craddock, P.R., Day, J.M.D., Valley, J.W., Dauphas, N., Taylor, L. A., 2010. Oxygen and iron isotope constraints on near-surface fractionation effects and the composition of lunar mare basalt source regions. Geochim. Cosmochim. Acta 74, 6249–6262 doi:10/dzbz7n.

Liu, P.-P., Zhou, M.-F., Luais, B., Cividini, D., Rollion-Bard, C., 2014. Disequilibrium iron isotopic fractionation during the high-temperature magmatic differentiation of the Baima Fe–Ti oxide-bearing mafic intrusion, SW China. Earth Planet. Sci. Lett. 399, 21–29. https://doi.org/10.1016/j.epsl.2014.05.002.

Lucey, P., 2006. Understanding the lunar surface and space-moon interactions. Rev. Mineral. Geochem. 60, 83–219. https://doi.org/10.2138/rmg.2006.60.2.

Luo, B., Wang, Z., Song, J., Qian, Y., He, Q., Li, Y., Head, J.W., Moynier, F., Xiao, L., Becker, H., Huang, B., Ruan, B., Hu, Y., Pan, F., Xu, C., Liu, W., Zong, K., Zhao, J., Zhang, W., Hu, Z., She, Z., Wu, X., Zhang, H., 2023. The magmatic architecture and evolution of the Chang'e-5 lunar basalts. Nat. Geosci. 16, 301–308. https://doi.org/10.1038/s41561-023-01146-x.

McKay, D.S., Fruland, R.M., Heiken, G.H., 1974. Grain size and the evolution of lunar soils. Lunar Planet. Sci. Conf. Proc. 1, 887–906.

Mckay, D.S., Heiken, G., Basu, A., Blanford, G., Simon, S., Reedy, R., French, B.M., Papike, J., 1991. The lunar regolith. In: Lunar Sourcebook. Cambridge University Press, Cambridge, UK, pp. 285–356.

Morris, R.V., 1976. Surface exposure indices of lunar soils: a comparative FMR study. Lunar Planet. Sci. Conf. Proc. 1, 315–335.

Morris, R., 1980. Origins and size distribution of metallic iron in the lunar regolith. In: Presented at the LUNAR AND PLANETARY SCIENCE XI, pp. 747–749. Abstract., pp. 747–749.

Oeser, M., Dohmen, R., Horn, I., Schuth, S., Weyer, S., 2015. Processes and time scales of magmatic evolution as revealed by Fe–mg chemical and isotopic zoning in natural olivines. Geochim. Cosmochim. Acta 154, 130–150. https://doi.org/10.1016/j.gca.2015.01.025.

Pernet-Fisher, J.F., Deloule, E., Joy, K.H., 2019. Evidence of chemical heterogeneity within lunar anorthosite parental magmas. Geochim. Cosmochim. Acta 266, 109–130. https://doi.org/10.1016/j.gca.2019.03.033.

Pieters, C.M., Noble, S.K., 2016. Space weathering on airless bodies: SPACE WEATHERING ON AIRLESS BODIES. J. Geophys. Res. Planets 121, 1865–1884. https://doi.org/10.1002/2016JE005128.

Poitrasson, F., Zambardi, T., Magna, T., Neal, C.R., 2019. A reassessment of the iron isotope composition of the moon and its implications for the accretion and differentiation of terrestrial planets. Geochim. Cosmochim. Acta 267, 257–274. https://doi.org/10.1016/j.gca.2019.09.035.

Prissel, K.B., Krawczynski, M.J., Nie, N.X., Dauphas, N., Aarons, S.M., Heard, A.W., Hu, M.Y., Alp, E.E., Zhao, J., 2024. Fractionation of iron and titanium isotopes by ilmenite and the isotopic compositions of lunar magma ocean cumulates. Geochim. Cosmochim. Acta 372, 154–170. https://doi.org/10.1016/j.gca.2024.01.006.

Qian, Y., Xiao, L., Head, J.W., Wöhler, C., Bugiolacchi, R., Wilhelm, T., Althoff, S., Ye, B., He, Q., Yuan, Y., Zhao, S., 2021. Copernican-aged (<200 Ma) impact ejecta at the Chang'e-5 landing site: statistical evidence from crater morphology, morphometry, and degradation models. Geophys. Res. Lett. 48. https://doi.org/10.1029/2021GL095341.

Qian, Y., Xiao, L., Zhao, J., Head, J.W., He, Q., Xu, H., Wang, F., Zhang, X., Ping, X., Zeng, W., Wang, X., Michalski, J., Liu, J., Ye, B., Wang, M., Sun, L., Pang, Y., Wang, J., Zhao, S., 2024. First magnetic and spectroscopic constraints on attenuated space weathering at the Chang'e-5 landing site. Icarus 410, 115892. https://doi.org/10.1016/j.icarus.2023.115892.

Shen, L., Zhao, R., Chang, C., Yu, J., Xiao, D., Bai, H., Zou, Z., Yang, M., Wang, W., 2024. Separate effects of irradiation and impacts on lunar metallic iron formation observed in Chang'e-5 samples. Nat. Astron. 8, 1110–1118. https://doi.org/10.1038/s41550-024-02300-0.

Shi, Q., He, Y., Zhu, J.-M., Wang, Y., Wang, Y., Wu, H., Wang, P., Yang, R., Sun, A., Zhang, Y., Wu, G., Wan, R., Lu, Z., Teng, F.-Z., Li, C., Yang, W., Zhang, C., Han, Z., Ke, S., 2024. Elemental differentiation and isotopic fractionation during space weathering of Chang'E-5 lunar soil. Geochim. Cosmochim. Acta 378, 127–143. https://doi.org/10.1016/j.gca.2024.06.011.

Sossi, P.A., Moynier, F., 2017. Chemical and isotopic kinship of iron in the earth and moon deduced from the lunar Mg-Suite. Earth Planet. Sci. Lett. 471, 125–135. https://doi.org/10.1016/j.epsl.2017.04.029.

Sossi, P.A., O'Neill, H.St.C., 2017. The effect of bonding environment on iron isotope fractionation between minerals at high temperature. Geochim. Cosmochim. Acta 196, 121–143. https://doi.org/10.1016/j.gca.2016.09.017.

Su, B., Zhang, D., Chen, Y., Yang, W., Mao, Q., Li, X.-H., Wu, F.-Y., 2023. Low Ni and co olivine in Chang'E-5 basalts reveals the origin of the young volcanism on the moon. Sci. Bull. 68, 1918–1927. https://doi.org/10.1016/j.scib.2023.07.020.

Taylor, L.A., Pieters, C.M., Keller, L.P., Morris, R.V., McKay, D.S., 2001. Lunar Mare soils: space weathering and the major effects of surface-correlated nanophase Fe. J. Geophys. Res. 106, 27985–27999. https://doi.org/10.1029/2000JE001402.

Taylor, L.A., Pieters, C., Patchen, A., Taylor, D.-H.S., Morris, R.V., Keller, L.P., McKay, D. S., 2010. Mineralogical and chemical characterization of lunar highland soils: insights into the space weathering of soils on airless bodies. J. Geophys. Res. Planets 115. https://doi.org/10.1029/2009JE003427.

Tian, Z., Jolliff, B.L., Korotev, R.L., Fegley, B., Lodders, K., Day, J.M.D., Chen, H., Wang, K., 2020a. Potassium isotopic composition of the Moon. Geochim. Cosmochim. Acta 280, 263–280. https://doi.org/10.1016/j.gca.2020.04.021.

Tian, H.-C., Zhang, C., Teng, F.-Z., Long, Y.-J., Li, S.-G., He, Y., Ke, S., Chen, X.-Y., Yang, W., 2020b. Diffusion-driven extreme mg and Fe isotope fractionation in Panzhihua ilmenite: implications for the origin of mafic intrusion. Geochim. Cosmochim. Acta 278, 361–375. https://doi.org/10.1016/j.gca.2019.10.004.

Tian, H.-C., Zhang, C., Yang, W., Du, J., Chen, Y., Xiao, Z., Mitchell, R.N., Hui, H., Changela, H.G., Zhang, T.-X., Tang, X., Zhang, D., Lin, Y., Li, X., Wu, F., 2023. Surges in volcanic activity on the moon about two billion years ago. Nat. Commun. 14, 3734. https://doi.org/10.1038/s41467-023-39418-0.

Wang, K., Moynier, F., Podosek, F.A., Foriel, J., 2012. An iron isotope perspective on the origin of the nanophase metallic iron in lunar regolith. Earth Planet. Sci. Lett. 337–338, 17–24. https://doi.org/10.1016/j.epsl.2012.05.021.

Wang, Z., Wang, W., Tian, W., Li, H., Qian, Y., Pei, J., Chen, Z., Wang, D., Liu, P.-P., Fa, W., Wu, J., Bao, H., 2023. Cooling rate of clinopyroxene reveals the thickness and effusion volume of Chang'E-5 basaltic flow units. Icarus 394, 115406. https://doi.org/10.1016/j.icarus.2022.115406.

Wang, Z., Zong, K., Li, Y., Li, J., He, Q., Zou, Z., Becker, H., Moynier, F., Day, J.M.D., Zhang, W., Qian, Y., Xiao, L., Hu, Z., She, Z., Hui, H., Wu, X., Liu, Y., 2024. Young KREEP-like mare volcanism from Oceanus Procellarum. Geochim. Cosmochim. Acta 373, 17–34. https://doi.org/10.1016/j.gca.2024.03.029.

Wiesli, A., Beard, B.L., Taylor, L.A., Johnson, C.M., 2003. Space weathering processes on airless bodies: Fe isotope fractionation in the lunar regolith. Earth Planet. Sci. Lett. 9. https://doi.org/10.1016/S0012-821X(03)00552-1.

Williams, H.M., Markowski, A., Quitté, G., Halliday, A.N., Teutsch, N., Levasseur, S., 2006. Fe isotope fractionation in iron meteorites: new insights into metal-sulphide segregation and planetary accretion. Earth Planet. Sci. Lett. 250, 486–500. https://doi.org/10.1016/j.epsl.2006.08.013.

Xian, H., Zhu, J., Yang, Y., Li, S., Lin, X., Xi, J., Xing, J., Wu, X., Yang, H., Zhou, Q., Tsuchiyama, A., He, H., Xu, Y.-G., 2023. Ubiquitous and progressively increasing ferric iron content on the lunar surfaces revealed by the Chang'e-5 sample. Nat. Astron. 7, 280–286. https://doi.org/10.1038/s41550-022-01855-0.

Xie, M., Xiao, Z., Xu, L., Fa, W., Xu, A., 2020. Change in the Earth–Moon impactor population at about 3.5 billion years ago. Nat. Astron. 5, 128–133. https://doi.org/10.1038/s41550-020-01241-8.

Xu, L., Yang, J.-H., Wang, H., Xie, L.-W., Yang, Y.-H., Huang, C., Wu, S.-T., 2022. Analytical feasibility of a new reference material (IRMM-524A Fe metal) for the in situ Fe isotopic analysis of pyrite and ilmenite without matrix effects by femtosecond LA-MC-ICP-MS. J. Anal. At. Spectrom. 37, 1835–1845.

Yang, W., Chen, Y., Wang, H., Tian, H.-C., Hui, H., Xiao, Z., Wu, S.-T., Zhang, D., Zhou, Q., Ma, H.-X., Zhang, C., Hu, S., Li, Q.-L., Lin, Y., Li, X.-H., Wu, F.-Y., 2022. Geochemistry of impact glasses in the Chang'e-5 regolith: constraints on impact melting and the petrogenesis of local basalt. Geochim. Cosmochim. Acta 335, 183–196. https://doi.org/10.1016/j.gca.2022.08.030.

Yao, Y., Xiao, C., Wang, P., Li, C., Zhou, Q., 2022. Instrumental neutron activation analysis of Chang'E-5 lunar regolith samples. J. Am. Chem. Soc. jacs.1c13604. https://doi.org/10.1021/jacs.1c13604.

Zeng, X., Li, X., Liu, J., 2023. Exotic clasts in Chang'e-5 regolith indicative of unexplored terrane on the moon. Nat. Astronomy 7, 152–159. https://doi.org/10.1038/s41550-022-01840-7.

Zhang, W., Hu, Z., Liu, Y., 2020. Iso-compass: new freeware software for isotopic data reduction of LA-MC-ICP-MS. J. Anal. At. Spectrom. 35, 1087–1096. https://doi.org/10.1039/D0JA00084A.

Zhang, L., Wang, C.-Y., Xian, H.-Y., Wang, J., Zhang, Y.-Q., Bao, Z., Lin, M., Xu, Y.-G., 2024. Large magnesium isotopic fractionation in lunar agglutinatic glasses caused by impact-induced chemical diffusion. Geochim. Cosmochim. Acta 378, 71–81. https://doi.org/10.1016/j.gca.2024.06.019.

Zong, K., Wang, Z., Li, J., He, Q., Li, Y., Becker, H., Zhang, W., Hu, Z., He, T., Cao, K., She, Z., Wu, X., Xiao, L., Liu, Y., 2022. Bulk compositions of the Chang'E-5 lunar soil: insights into chemical homogeneity, exotic addition, and origin of landing site basalts. Geochim. Cosmochim. Acta S0016703722003258. https://doi.org/10.1016/j.gca.2022.06.037.